Antiferromagnetic Ordering in Superconducting $YBa_2Cu_3O_{6.5}$

Y. Sidis,[1] C. Ulrich,[2] P. Bourges,[1] C. Bernhard,[2] C. Niedermayer,[3] L. P. Regnault,[4] N. H. Andersen,[5] and B. Keimer[2]

[1]*Laboratoire Léon Brillouin, CEA-CNRS, CE Saclay, 91191 Gif sur Yvette, France*
[2]*Max-Planck-Institut für Festkörperforschung, 70569 Stuttgart, Germany*
[3]*University of Konstanz, 78434 Konstanz, Germany*
[4]*Département de Recherche Fondamentale sur la matière Condensée, CEA Grenoble, 38054 Grenoble Cedex 9, France*
[5]*Condensed Matter Physics and Chemistry Department, Risø National Laboratory, DK-4000 Roskilde, Denmark*

(Received 8 January 2001)

Commensurate antiferromagnetic ordering has been observed in the superconducting high-T_c cuprate $YBa_2Cu_3O_{6.5}$ ($T_c = 55$ K) by polarized and unpolarized elastic neutron scattering. The magnetic peak intensity exhibits a marked enhancement at T_c. Zero-field muon-spin-resonance experiments demonstrate that the staggered magnetization is not truly static but fluctuates on a nanosecond time scale. These results point towards an unusual spin density wave state coexisting with superconductivity.

DOI: 10.1103/PhysRevLett.86.4100 PACS numbers: 74.25.Ha, 74.72.–h, 76.75.+i

The coexistence of superconductivity with an antiferromagnetic (AF) state has recently been reported in certain Ce based heavy fermion systems under pressure [1], inspiring theories of spin fluctuation mediated pairing of electrons in these systems. In contrast, the antiferromagnetic and superconducting phases of the copper oxide high-T_c superconductors are generally considered to be well separated. However, since the early days of high temperature superconductivity, there have been persistent reports of local magnetic moments in the metallic and superconducting regimes of the phase diagram. Specifically, zero-field muon-spin-resonance (ZF-μSR) measurements [2,3] in both $La_{2-x}Sr_xCuO_4$ and $Y_{1-x}Ca_xBa_2Cu_3O_6$ compounds provide indications of a microscopic coexistence of superconductivity ($T_c \leq 50$ K) and frozen magnetic moments at low temperature ($T \leq 10$ K), and Mössbauer spectroscopy shows low temperature spin freezing up to $x \leq 0.66$ in $YBa_2Cu_3O_{6+x}$ [4]. Both μSR and Mössbauer spectroscopies are local probes that provide no information about the spatial correlations of the magnetic moments. An early observation of coexistence between superconductivity and antiferromagnetism from neutron measurements in $YBa_2Cu_3O_{6.55}$ has remained unconfirmed [5]. More recently, an incommensurate magnetic ordering below a critical temperature T_m has been observed by elastic neutron scattering in La_2CuO_4-family superconductors [6]. Interestingly, this magnetic phase coexists with superconductivity in a certain doping range. In superoxygenated $LaCuO_{4+\delta}$, T_m and T_c are actually identical ($T_c = 42$ K), whereas T_m remains larger than T_c in $La_{1.6-x}Nd_{0.4}Sr_xCuO_{4+\delta}$ compounds for $x \leq 0.2$.

Here we report the observation, by neutron scattering, of *commensurate* AF order in the superconducting compound $YBa_2Cu_3O_{6.5}$ ($T_c = 55$ K), using polarized and unpolarized elastic neutron scattering. This AF order develops at a high temperature ($T_N = 310$ K) and is characterized by a large correlation length around 100 Å, but the low temperature staggered magnetization remains weak, $m_0 = 0.05\mu_B$. Observation of such a small moment with a large T_N is reminiscent of a spin-density wave (SDW) state observed in itinerant magnets [7]. Interestingly, the magnetic signal around the AF Bragg reflections exhibits a significant enhancement at T_c. Finally, ZF-μSR measurements carried out on the same sample show that the AF staggered magnetization is not truly static but fluctuates with a characteristic frequency in the μeV range.

The experiments were performed on a large $YBa_2Cu_3O_{6.5}$ single crystal (~23 g) grown using the top seed melt texturing method [8]. The sample was subsequently annealed to achieve an oxygen concentration of $x = 0.5$ [9]. We checked by neutron measurements at room temperature the presence of the $Q = (2.5, 0, 5)$ Bragg peak characteristic of the *orthorhombic*-II phase [9] and derive the correlation lengths: $\xi_{ab} \simeq 20$ Å and $\xi_c \simeq 12$ Å. This demonstrates well ordered CuO chains and hence uniform hole doping within the CuO_2 planes. The sample displays a sharp superconducting transition at $T_c = 55$ K, measured by a bulk-sensitive neutron depolarization technique [8]. Neutron scattering experiments were carried out on the 4F1 and 4F2 cold triple axis spectrometers at the reactor Orphée in Saclay (France). These spectrometers are equipped with double monochromators consisting of two pyrolithic graphite (PG) crystals whose (002) reflections were set to select the incident wave vector $k_I = 1.48$ Å^{-1}. For unpolarized neutron scattering measurements we used a PG(002) analyzer. Two filters, Be and PG, were used to remove higher order contamination. Polarized neutron scattering experiments were performed with a bender to polarize the incident beam and with a Heusler (111) analyzer. A conventional polarized neutron setup [10] was used with a flipper in the scattered beam to rotate the neutron spin polarization by 180° and a magnetic guide field **H** to preserve the neutron polarization. The (110) and (001) directions of reciprocal space were within the horizontal scattering plane. We quote the scattering vector $\mathbf{Q} = (H, K, L)$ in units of the reciprocal lattice vectors $\mathbf{a}^* \sim \mathbf{b}^* = 1.63$ Å^{-1} and $\mathbf{c}^* = 0.53$ Å^{-1}.

 0031-9007/01/86(18)/4100(4)$15.00

The elastic signal was discovered in the course of unpolarized elastic neutron scattering experiments on superconducting $YBa_2Cu_3O_{6.5}$ around the wave vectors $\mathbf{Q} = (0.5, 0.5, L)$ for the $L \neq 0$ integer. The structure factor of this diffraction pattern is identical to that of the undoped AF parent compound $YBa_2Cu_3O_6$. Figure 1a shows the temperature dependence of the intensity measured at two of these wave vectors: $L = 1, 2$. The strong temperature dependence, as well as the presence of two filters in the beam, ensures that the signal is not due to $\lambda/2$ contamination, and extensive polarized beam experiments (below) demonstrate that the signal is indeed of magnetic origin. The intensity exhibits a sharp onset at a "Néel" temperature of $T_N = 310$ K. From T_N down to $T_c = 55$ K, the magnetic intensity continuously increases, following the power law: $(1 - T/T_N)^{2\beta}$ with $\beta = 0.25$ (dashed line in Fig. 1a). Surprisingly, another marked upturn of the AF intensity is observed at the *superconducting* transition temperature T_c (Fig. 1b). After calibration against nuclear Bragg reflections, the staggered moment at $T = 60$ K is found to be $m_0 \sim 0.05\mu_B$ (assuming a homogeneous distribution of the magnetic moments at all copper sites in the plane), that is, more than an order of magnitude smaller than in the insulating parent compound $YBa_2Cu_3O_6$ [11,12]. The small moment (which translates into an elastic magnetic cross section more than 2 orders of magnitude smaller than that of $YBa_2Cu_3O_6$) explains why the signal could not be measured in previous neutron measurements on smaller samples.

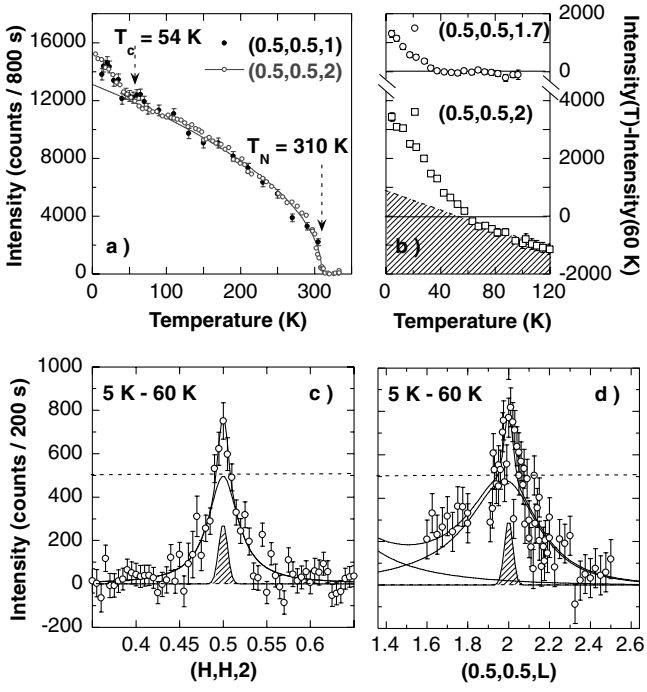

FIG. 1. (a) Temperature dependence of the magnetic intensity measured at $\mathbf{Q} = (0.5, 0.5, 2)$ (with an unpolarized beam) and $(0.5, 0.5, 1)$ (with a polarized beam) scaled to each other. From $T_N = 310$ K down to $T_c = 55$ K, the magnetic intensity increases as a power law (dashed line). (b) Enhancement of the low temperature static magnetic response at $\mathbf{Q} = (0.5, 0.5, 2)$ and $(0.5, 0.5, 1.7)$ with respect to the magnetic scattering at 60 K. The dashed line and the shaded area extrapolate down to low temperature the temperature dependence of the $(0.5, 0.5, 2)$ magnetic Bragg reflection as measured above T_c [panel (a)]. (c),(d) Difference between scans at $T = 5$ K and $T = 60$ K measured around $(0.5, 0.5, 2)$ along (110) and (001), respectively.

We next describe polarized beam experiments designed to confirm the magnetic origin of the signal and to determine the moment direction. The matrix element for magnetic neutron scattering can be written as [13]

$$\langle m'|\vec{\sigma} \cdot \vec{M}_\perp|m\rangle, \tag{1}$$

where $|m\rangle, |m'\rangle = |\pm\frac{1}{2}\rangle$ are the initial and final states of the neutron spin, $\vec{\sigma}$ is the neutron spin Pauli matrix, and $\vec{M}_\perp$ is the component of the electronic magnetic moment perpendicular to the scattering vector $\mathbf{Q}$. Note that the functional form of the matrix element does not depend on whether $\vec{M}$ originates in the spin or the orbital motion of the electrons. The direction of the neutron spin quantization axis at the sample position is selected by a small guide field $\mathbf{H}$. From Eq. (1) one sees that the magnetic intensity is entirely spin-flip (SF) when $\mathbf{H} \parallel \mathbf{Q}$. When $\mathbf{H} \perp \mathbf{Q}$, on the other hand, the ratio of magnetic intensities in SF and non-spin-flip (NSF) channels depends on the orientation of $\vec{M}$.

Figures 2a–2d show rocking scans performed around $\mathbf{Q} = (0.5, 0.5, 1)$ at $T = 60$ K. The two-peak profile is due to two crystallographic grains in our sample (a rocking scan through a nuclear reflection with the same profile is shown in the inset). For $\mathbf{H} \parallel \mathbf{Q}$ a peak is seen only in the SF channel (Fig. 2a), while the measured scattering intensity in the NSF channel remains featureless (Fig. 2b). This proves that the observed signal is of magnetic origin. The results for $\mathbf{H} \perp \mathbf{Q}$ in Figs. 2c and 2d then provide information about the orientation of the magnetic moments. The full elastic magnetic cross section is proportional to $\frac{1}{2}\langle M\rangle^2_{a,b}(1 + \sin^2\theta_l) + \langle M\rangle^2_c \cos^2\theta_l$, where θ_l stands for the angle between $\mathbf{Q}$ and the (110) direction [$\theta_l = 25°$ for $\mathbf{Q} = (0.5, 0.5, 1)$], and $\langle M\rangle_{a,b}$ and $\langle M\rangle_c$ represent the thermodynamic averages of the magnetization within the a, b plane and perpendicular to it, respectively. (Note that a and b directions are superposed in our experiment due to twinning.) For $\mathbf{H}$ along $(1\bar{1}0)$ perpendicular to the scattering plane (Figs. 2c and 2d), this intensity is apportioned such that the SF channel measures $\langle M\rangle^2_{a,b}\frac{1}{2}\sin^2\theta_l + \langle M\rangle^2_c \cos^2\theta_l$ and the NSF channel measures $\frac{1}{2}\langle M\rangle^2_{a,b}$. The weak intensity observed in the SF channel (Fig. 2c) and the larger intensity in the NSF channel demonstrate that the magnetic moments are predominantly within the basal a, b plane. Additional measurements with $\mathbf{H} \perp \mathbf{Q}$ but for $\mathbf{H}$ in the scattering plane corroborate this conclusion.

Both the moment direction and the structure factor of the magnetic order observed in $YBa_2Cu_3O_{6.5}$ are thus similar to those of the undoped parent compound. One possible interpretation of this observation, namely, macroscopic or mesoscopic concentration gradients of oxygen leading to

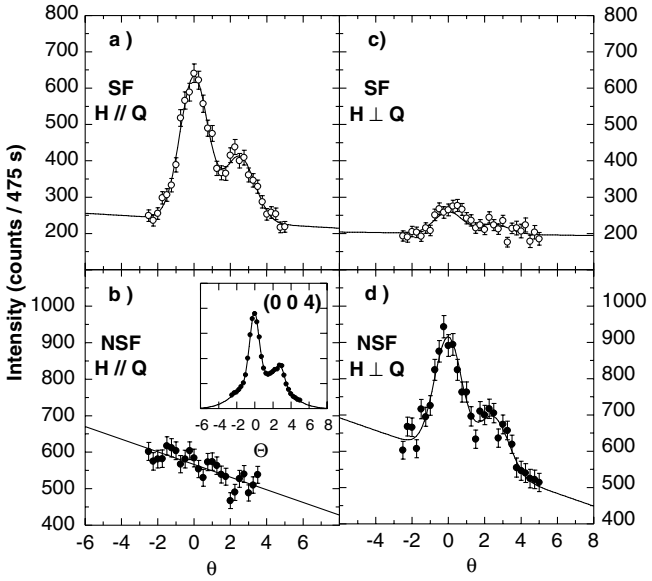

FIG. 2. Polarized neutron scattering measurements at $T = 60$ K, showing rocking scans at $\mathbf{Q} = (0.5, 0.5, 1)$ in both SF and NSF channels for two different magnetic guide field directions (see text). The inset shows a rocking scan at the nuclear Bragg reflection $(1, 1, 0)$, measured by unpolarized neutron scattering. The double peak structure originates from two distinct crystallites in the sample.

an inhomogeneous charge distribution, can be ruled out. First, the shapes of the rocking curves around the AF Bragg reflections (Figs. 2a, 2c, and 2d) exactly reproduce those of the nuclear Bragg reflections (inset in Fig. 2b). The observed double peak structure originates from two distinct grains in our sample, which are separated by a tilt angle of 2.5°. The volume ratio of these grains is found the same for structural and magnetic scattering, ruling out phase segregation where magnetic order occurs only in a small part of the sample. Second, we observe a sharp transition with $T_N = 310$ K, whereas in the case of an inhomogeneous sample one would expect a broad distribution of transition temperatures starting from $T_N = 410$ K, the Néel temperature of the undoped compound. Conversely, the superconducting transition of our sample measured by a bulk-sensitive technique is also very sharp. Third, we observe a marked increase of the magnetic intensity at T_c; a minority phase of the undoped compound would not be affected by superconductivity. Finally, while the Néel state in the undoped insulator is associated with a static staggered magnetization, the μSR measurements described below show that such a static moment is absent in $YBa_2Cu_3O_{6.5}$. These observations imply the absence of large-scale inhomogeneities in our sample.

A quantitative analysis of Figs. 2a and 2d reveals a systematic broadening of the rocking curve around the AF Bragg reflection $\mathbf{Q} = (0.5, 0.5, 1)$ with respect to the nuclear one, indicating finite size AF correlations. At 60 K, an anisotropic correlation length, $\xi_a \simeq 20a$ and $\xi_c \simeq 9c$, is determined from scans along (110) and (001) around the AF Bragg reflections. From 60 K up to T_N, these correlation lengths remain constant within the error bars. At 60 K, the intensity ratio (peak amplitude) between the AF Bragg reflections $I(L = 1)/I(L = 2) = 0.67 \pm 0.05$ is somewhat larger than expected for localized $(d_{x^2-y^2})$ Cu spins aligned in the plane [12,14]. The analysis of the magnetic structure factor over several AF peaks (not presented here) actually shows a form factor decreasing faster at large $|Q|$, consistent with more delocalized magnetic states.

Below T_c, we observe a pronounced *broadening* of the magnetic reflections that goes along with the upturn in the peak intensity. We have performed scans around $\mathbf{Q} = (0.5, 0.5, 2)$ along both the (110) and the (001) directions at $T = 5$ K and $T = 60$ K whose differences are reported in Fig. 1c and Fig. 1d, respectively. The additional low temperature intensity remains centered at $\mathbf{Q} = (0.5, 0.5, 2)$, but because of the broadening it becomes observable all along $\mathbf{Q} = (0.5, 0.5, L)$, for instance, at $\mathbf{Q} = (0.5, 0.5, 1.7)$ as shown in Fig. 1b. The observed momentum broadening cannot simply be attributed to a decrease of the AF correlation length in the superconducting phase, because the peak intensity at $\mathbf{Q} = (0.5, 0.5, 2)$ intensity shows an *upturn* below T_c, rather than the downturn expected if the integrated intensity remained constant. It is therefore more appropriate to consider the development of a second type of AF order (with much shorter correlation length) below T_c, in addition to the one already present in the normal state. Figures 1c and 1d have thus been fitted as a superposition of two contributions centered at the wave vector $\mathbf{Q} = (0.5, 0.5, 2)$. The sharper one, with a Gaussian profile with $\Delta q = 0.0135$ Å^{-1}, corresponds to the continuous increase of the magnetic response observed above T_c (shaded peaks in Figs. 1c and 1d). The second contribution, with a broader Lorentzian profile, is characterized by an onset at T_c and an anisotropic correlation length: $\xi_{ab} \simeq 22$ Å ($\Delta q = 0.02$ Å^{-1}, Fig. 1c) and $\xi_c \simeq 9$ Å ($\Delta q = 0.046$ Å^{-1}, Fig. 1d). It is noteworthy that the superconducting coherence length, ξ^{SC}, in high-T_c superconductors is similarly anisotropic; in particular $\xi^{SC}_{ab} \sim 20$ Å and $\xi^{SC}_c \sim 3$–7 Å [15] in $YBa_2Cu_3O_{6+x}$. The second order parameter below T_c accounts for only 15% of the overall magnetic peak intensity (Fig. 1a), but because of its broader structure in q space its integrated intensity ($\sim 0.07\mu_B$) is comparable to that of the first component above T_c.

Additional higher resolution (smaller k_I) measurements show that the signal remains resolution limited in energy when the resolution is tightened to ~ 50 μeV. Thus, the observed AF order appears static on a time scale shorter than $\sim 10^{-10}$ s. In order to obtain sensitivity to spin fluctuations on a larger time scale, ZF-μSR measurements were performed at the GPS beam line of the Paul-Scherrer-Institute in Villigen, Switzerland, on a piece cut from the same sample. For $T > 60$ K only a very slow depolarization of the muon spin polarization $P(t)$ is observed which is due to the nuclear Cu moments and is well described by a Kubo-Gauss function (KG) with a damping rate of 0.12 μs^{-1} [3]. Static AF ordered

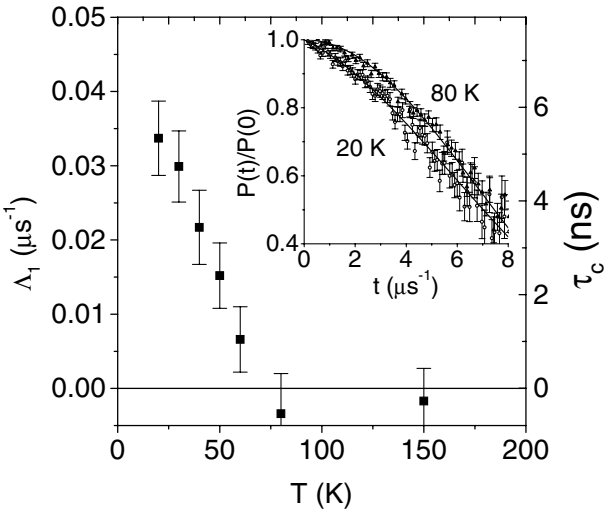

FIG. 3. Temperature dependence of the ZF-μSR relaxation rate Λ_1 (left scale) and relaxation rate of the magnetic moments τ_c (right scale). Inset: Time dependent muon-spin polarization at $T = 20$ and 80 K.

moments of size $0.05\mu_B$ (as indicated by the neutron data) should give rise to an oscillating signal with a precession frequency of about 0.4 MHz, that is, about 1/10 the value that is typically observed in $YBa_2Cu_3O_6$ [3]. Even under the assumption that these static electronic magnetic moments are strongly disordered, we should still observe a rapid depolarization with a rate of $\Lambda_1 \sim 2.5\ \mu s^{-1}$. The circumstance that this is clearly not observed implies that the magnetic moments fluctuate on a time scale longer than the one of the neutron scattering experiment (10^{-10} s) but much shorter than the one of the μSR experiment (10^{-6} s). As shown in the inset of Fig. 3, the depolarization becomes somewhat faster at low temperatures, and the shape of $P(t)$ gradually changes from Gaussian to exponential. The inset in Fig. 3 shows the result of a fit using the function $P(t) = P(0) \times \mathrm{KG} \times \exp(-\Lambda_1 t)$. The KG function describes the contribution of the nuclear Cu moments which should be T independent; the KG depolarization rate thus has been fixed to the value at 150 K, i.e., 0.12 μs^{-1}. The exponential function describes the depolarization due to the rapidly fluctuating electronic moments. Figure 3 shows the T dependence of Λ_1 as given by the scale on the left hand side. For the limit of rapidly fluctuating moments having a characteristic relaxation rate τ_c ($\gamma_\mu B_\mu \ll \tau_c$) and under the assumption that the field $B_\mu \approx 40$ G at the muon site is determined by the neutron scattering measurements above, we obtain $\tau_c = \Lambda_1/(\gamma_\mu B_\mu)^2 = \Lambda_1/6.3$ [μs] as shown by the scale on the right hand side of Fig. 3.

In summary, an unusual commensurate AF phase, with in-plane magnetic moments fluctuating on a nanosecond time scale, is found to coexist with superconductivity in $YBa_2Cu_3O_{6.5}$. As in itinerant magnetic systems [7], we observe a small value of the ordered moment ($\sim 0.05\mu_B$ at $T = 60$ K) together with a large $T_N = 310$ K. The observed commensurate structure is not compatible with stripe ordering whose structure in momentum space is incommensurate. A disorder-induced AF long-range ordered state with spatially inhomogeneous local moment has been predicted in the spin gap phase of the cuprates [16]. The coexistence of an AF SDW state and d-wave superconductivity has also been considered theoretically [17–19]. It has been shown that when both states coexist there are unusual coherence effects and a π-triplet superconducting order parameter appears at T_c (when $T_c \leq T_N$). Electrons in the superconducting condensate may thus contribute the unusual neutron scattering response we observe below T_c. Finally, it was shown very recently that the staggered orbital current patterns proposed earlier [20] can produce in-plane magnetic moments under certain conditions [21].

We acknowledge stimulating discussions with S. Chakravarty, J. Hodges, G. Khaliullin, F. Onufrieva, and P. Pfeuty.

[1] N. D. Mathur *et al.,* Nature (London) **394**, 39 (1998).
[2] A. Weidinger *et al.,* Phys. Rev. Lett. **62**, 102 (1989); R. F. Kiefl *et al., ibid.* **63**, 2136 (1989).
[3] C. Niedermayer *et al.,* Phys. Rev. Lett. **80**, 3843 (1998).
[4] J. A. Hodges *et al.,* Physica (Amsterdam) **184C**, 270 (1991).
[5] D. Petitgrand *et al.,* J. Phys. (Paris) **49**, 1815 (1988).
[6] Y. S. Lee *et al.,* Phys. Rev. B **60**, 3643 (1999); J. M. Tranquada *et al., ibid.* **59**, 14 712 (1999).
[7] T. Moriya, *Spin Fluctuations in Itinerant Electron Magnetism,* Springer Series in Solid-State Sciences Vol. 56 (Springer-Verlag, Berlin, 1985).
[8] H. F. Fong *et al.,* Phys. Rev. B **61**, 14 773 (2000).
[9] N. H. Andersen *et al.,* Physica (Amsterdam) **317C–318C**, 259 (1999).
[10] R. M. Moon *et al.,* Phys. Rev. **181**, 920 (1969).
[11] M. J. Jurgens *et al.,* Physica (Amsterdam) **156B–157B**, 846 (1989).
[12] S. Shamoto *et al.,* Phys. Rev. B **48**, 13 817 (1993).
[13] S. M. Lovesey, *Theory of Thermal Neutron Scattering* (Oxford University Press, Oxford, 1985).
[14] J. Rossat-Mignod *et al.,* in *Selected Topics in Superconductivity,* edited by L. C. Gupta and M. S. Multani, Frontiers in Solid State Sciences Vol. 1 (World Scientific, Singapore, 1993), p. 265.
[15] See, e.g., *Physical Properties of High Temperature Superconductors I and II,* edited by D. M. Ginsberg (World Scientific, Singapore, 1989).
[16] H. Fukuyama, J. Phys. Chem. Solids **60**, 1003 (1999); H. Kohno *et al.,* J. Phys. Soc. Jpn. **68**, 1500 (1999).
[17] M. Murakani and H. Fukuyama, J. Phys. Soc. Jpn. **67**, 41 (1998); B. Kyung, Phys. Rev. B **62**, 9083 (2000).
[18] F. Bouis *et al.,* Physica (Amsterdam) **284B–288B**, 677 (2000).
[19] S. C. Zhang *et al.,* Phys. Rev. B **60**, 13 070 (1999); A. I. Lichtenstein and M. I. Katsnelson, *ibid.* **62**, R9283 (2000); F. F. Assaad and M. Imada, *ibid.* **58**, 1845 (1998); M. Vojta and S. Sachdev, Phys. Rev. Lett. **83**, 3916 (1999).
[20] S. Chakravarty *et al.,* Phys. Rev. B (to be published), cond-mat/0005443.
[21] S. Chakravarty *et al.,* e-print cond-mat/0101204.